Proceedings of Meetings on Acoustics

JUNE 29 2026

Quantitative Lung Ultrasound Biomarkers for Automatic Stratification of Idiopathic Pulmonary Fibrosis: an *in-vivo* study

Mattia Perpenti ; Federico Mento ; Alessandro Perrotta; Giovanni Pierro; Tiziano Perrone; Andrea Smargiassi; Riccardo Inchingolo; Libertario Demi

Proc. Mtgs. Acoust. 60, 020003 (2025)
https://doi.org/10.1121/2.0002340

Connected Content

This is a companion to: Real-time and automatic lung diagnostics by quantitative lung ultrasound spectroscopy, a multicenter study

Proceedings of Meetings on Acoustics

Volume 60 http://acousticalsociety.org/

Sixth Joint Meeting
189th Meeting of the Acoustical Society of America and the Acoustical Society of Japan

Honolulu, Hawaii
1-5 December 2025

Biomedical Acoustics: Paper 2aBAa4

Quantitative Lung Ultrasound Biomarkers for Automatic Stratification of Idiopathic Pulmonary Fibrosis: an *in-vivo* study

Mattia Perpenti
Department of Information and Communication Engineering, University of Trento Department of Information Engineering and Computer Science: Universita degli Studi di Trento Dipartimento di Ingegneria e Scienza dell'Informazione, Trento, TN, 38123, ITALY; mattia.perpenti@unitn.it

Federico Mento
University of Trento: Universita degli Studi di Trento, Trento, 38123, ITALY; federico.mento@unitn.it

Alessandro Perrotta and Giovanni Pierro
Policlinico Universitario Agostino Gemelli, Rome, ITALY; alessandroperrotta1992@gmail.com; gpierro33@gmail.com

Tiziano Perrone
Humanitas Gavazzeni, Bergamo, ITALY; tiziano.perrone@gavazzeni.it

Andrea Smargiassi and Riccardo Inchingolo
Policlinico Universitario Agostino Gemelli, Rome, ITALY; andrea.smargiassi@policlinicogemelli.it; riccardo.inchingolo@policlinicogemelli.it

Libertario Demi
Universita degli Studi di Trento, Trento, 38123, ITALY; libertario.demi@unitn.it

Idiopathic pulmonary fibrosis (IPF) is a progressive lung pathology that can occur in two distinct stages: chronic IPF and acute IPF exacerbation (IPFE). Although their histological conditions differ, their stratification through gold standard lung imaging remains challenging. Quantitative lung ultrasound (Q-LUS) has recently emerged as a promising, safe, and non-invasive imaging modality for characterizing the lung condition. Previous studies analyzed the frequency dependence of imaging artifacts features from different pathologies to enhance diagnostic specificity. However, these studies marginally explored IPF stratification, analyzing the mean values of specific spectral biomarkers computed over the lung ultrasound (LUS) scans of a patient. In this study, LUS images from a cohort of 32 patients with IPF are segmented and quantified into 12 spectral biomarkers with a fully automatic segmentation algorithm. Rather than compressing each spectral biomarker to its mean value, a deeper analysis of their distribution is performed. Five statistical parameters (minimum, 25th, 50th, and 75th percentile, and maximum) are derived for each spectral biomarker, yielding to 60 parameters per patient. Parameters are ranked by statistical significance to train nested k-fold Naïve Bayes classifiers. This method is compared with state-of-art approach, demonstrating accuracies improvement up to 13% in IPF stratification.

Proceedings of Meetings on Acoustics, Vol. 60, 020003 (2026); https://doi.org/10.1121/2.0002340.

1. INTRODUCTION

Idiopathic Pulmonary Fibrosis (IPF) is a progressive disease that can evolve into two distinct histological stages: a relentless chronic progression and a sudden acute exacerbation (IPFE).[1,2] Although these two stages fall within the same disease, their histopathological conditions differ.[2,3] Chronic IPF manifests heterogeneous fibrotic tissues at the pleural and paraseptal regions, leading to dense scars and cystic airspaces.[1–3] IPFE manifests as diffuse sudden alveolar damage that evolve into interstitial infiltrations and leads to the formation of acellular membranes along the alveolar walls, often resulting fatal to the patient.[1–3] IPF diagnosis and monitoring are key factors to undertake a therapeutic strategy that slowdown the progression of the disease.[4] Lung imaging is an essential tool employed in the clinical diagnosis and monitoring of lung pathologies. Yet, modern imaging tools (e.g., computed tomography) exhibit low specificity and expose to ionizing radiation.[5,6] Additionally, they are not always accessible, as they may endanger patients in critical conditions. More accessible and safer imaging alternatives include lung ultrasound (LUS).[7] However, LUS is limited to the evaluation of the lung surface, as the aerated structures of the lung hinder ultrasound wave propagation.[7–9] Standard LUS analyses are in fact restricted to the subjective detection and interpretation of imaging patterns [e.g., vertical artifacts and pleural line (PL)].[7] This approach lacks diagnostic specificity and is poorly reproducible, thereby underutilizing LUS potential. Quantitative lung ultrasound (Q-LUS) spectroscopy was designed to overcome LUS limitations, providing both improved diagnostic specificity and reproducibility.[6,8,10–14] With Q-LUS, the frequency dependence of LUS imaging pattern biomarker is analyzed to enhance diagnostic specificity.[4,15–17] Spectral biomarker from patients affected by chronic IPF and IPFE were previously analyzed by quantifying PL and artifactual patterns.[18,19] Specifically, a dedicated acquisition method was proposed, in which ten areas were scanned. For each area a video at multiple frequencies is obtained. From each video, the mean of a spectral biomarker is obtained and then averaged across an exam, yielding to a single mean value for each patient. Since different pathologies affect the lung in a rather complex way, including potentially spatial distribution across the lung,[20] the mean, although worthed to be investigated as first statistical parameter, may be insufficient to perform optimal stratification.

In this work, we investigate whether a deeper analysis of the spectral biomarker distribution improves stratification specificity of chronic IPF and IPFE. Data are acquired from a cohort of 32 patients diagnosed with IPF. For each patient, ten areas were scanned, composing a video of 23 multifrequency images. The images were automatically segmented into three regions: pre-pleura, pleura, and artifactual region by means of an automatic segmentation algorithm of the pleural line (ASAP).[19] The regions are used to extract 5 frequency-dependent I_{TOT} quantities and, from 4 of them (see Fig. 1), three spectral biomarkers are extracted from each quantity: $\max_f I_{\mathrm{TOT}}$, center frequency, bandwidth, obtaining a total of 12 spectral biomarkers for each LUS image.[19] The distribution of each spectral biomarker is analyzed by means of 5 statistical parameters: minimum, 25^{th}, 50^{th}, and 75^{th} percentile, and maximum, characterizing each patient by means of 60 statistical parameters (5 statistical parameters $\times$ 12 spectral biomarkers). The obtained parameters are ranked by significance and used to train a nested Naive Bayes classifier by means of an incremental number of input parameters. Stratification performance are analyzed in terms of accuracy, specificity, and sensitivity and compared with the State-of-the-Art (SoA) approach.

2. METHODS

This is a single-center, observational diagnostic study conducted in the context of the SAURON study, in collaboration with the Agostino Gemelli Hospital of Rome (approved by the Ethical Committee of the Fondazione Policlino Universitario Gemelli IRCCS in Rome, protocol 0002865/22, ID 4710).[19]

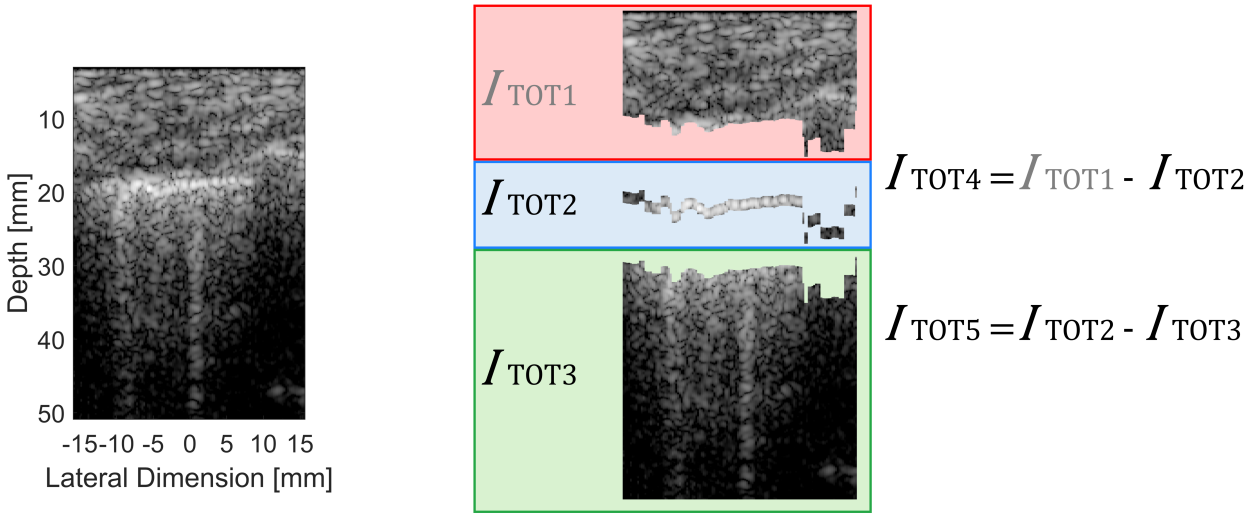

Figure 1: Segmentation of a LUS image. On the left, a LUS image before segmentation, on the right, LUS image segmented into pre-pleura (red rectangle), PL (light blue rectangle), and artifactual region (green rectangle), quantified into I_{TOT1}***,*** I_{TOT2}***, and*** I_{TOT3}***, respectively. Additionally, the ratios*** I_{TOT4} ***and*** I_{TOT5} ***are represented.*** I_{TOT1} ***is represented in gray color, as spectral biomarkers were not extracted from it.***

A. DATASET

Radiofrequency LUS data were acquired with an ULA-OP programmable research scanner[21] connected to an LA523 (Esaote, Florence, Italy) linear probe (192 elements, $245\,\mu\mathrm{m}$ pitch). The scanner was programmed to transmit and receive signals using a 64-element sub-aperture. In transmission, a $2\,\mu\mathrm{s}$ pulse was transmitted at 3, 4, 5, and $6\,\mathrm{MHz}$ of center frequency, thus guaranteeing each subband to have a narrow bandwidth ($1\,\mathrm{MHz}$ at $-10\,\mathrm{dB}$).[4,8,22] The focal point was centered at PL ($\approx 2\,\mathrm{cm}$). The received signal is digitize using a sampling frequency of $50\,\mathrm{MHz}$.[4] The images were thus formed by 129 lines. A speed of sound of $1546\,\frac{\mathrm{m}}{\mathrm{s}}$ was assumed for the time-to-space conversion (along depth).[4] Data were acquired following a standardized acquisition protocol.[23] Ten areas were scanned and cine-loops of 23 multifrequency images were stored. By "multifrequency image" we refer to the same region acquired at four different center frequencies.

Data were acquired from a cohort of 32 patients affected by IPF, from which 20 patients were staged as chronic IPF (172 cine-loops stored for a total of 3944 multifrequency images) and 12 as IPFE (110 cine-loops stored for a total of 2530 multifrequency images). Diagnosis were confirmed thanks to standard clinical examinations.

B. PATTERN SEGMENTATION

To enable quantification, LUS imaging patterns are segmented in a two-step process as follows: Step 1, unwanted frequency components of all the multifrequency images are removed with a 12^{th} order Butterworth filter ($1.8\,\mathrm{MHz}$ bandwidth) centred at the respective center frequency; step 2, the signal envelope is extracted by means of the Hilbert transform and normalized with respect to its maximum value. Thereafter, LUS images are segmented into three regions: (i) the pre-pleura region, corresponding to the intercostal tissue layer, which does not provide information on the lung; (ii) PL, which does not represent the anatomical PL (composed of visceral and parietal pleura), but the acoustic interface between the intercostal tissues and the aerated structures of the lung; and (iii) the artifactual region, which represents the area deeper than PL, where imaging artifacts can be observed.

Table 1: List of the biomarker p-values grouped by I_{TOT} regions. p-values are highlighted by a color map from green (significant) to red (non-significant).

	I_{TOT2}		I_{TOT3}		I_{TOT4}		I_{TOT5}	
	Qty.	*p-value*	Qty.	*p-value*	Qty.	*p-value*	Qty.	*p-value*
maxI	MIN	0.2498	MIN	0.1620	MIN	0.3762	MIN	0.0519
	P25	0.8510	P25	0.1663	P25	0.0662	P25	0.0344
	P50	0.8229	P50	0.0486	P50	0.0794	P50	0.0155
	P75	0.5394	P75	0.0291	P75	0.2911	P75	0.1293
	MAX	0.3164	MAX	0.0012	MAX	0.4022	MAX	0.6740
CF	MIN	1	MIN	0.4476	MIN	0.4847	MIN	1
	P25	0.1283	P25	0.9646	P25	0.5001	P25	1
	P50	0.5199	P50	0.7224	P50	0.4494	P50	0.5958
	P75	0.8961	P75	1	P75	1	P75	0.1039
	MAX	1	MAX	1	MAX	1	MAX	0.0830
BW	MIN	0.7369	MIN	0.4486	MIN	0.9785	MIN	0.9444
	P25	0.4658	P25	1	P25	0.5340	P25	0.5283
	P50	0.8034	P50	0.9410	P50	0.3645	P50	0.2157
	P75	0.4672	P75	0.6959	P75	0.2849	P75	0.1530
	MAX	1	MAX	1	MAX	1	MAX	0.4476

Abbreviations: MaxI = $\max_f I_{\mathrm{TOT}}$; CF = Center Frequency; BW = Bandwidth.

These three regions are segmented by means of a fully automated segmentation algorithm of PL (ASAP), optimized, tested, and presented in a previous study.[19] ASAP segments a LUS image into the three mentioned regions by detecting PL.[19]

C. QUANTIFICATION AND STATISTICAL PARAMETERS

The three LUS regions segmented in Sec. 2.B are quantified into five quantities. Three quantities are obtained from the computation of the total intensity, respectively, I_{TOT1}, I_{TOT2}, I_{TOT3} for pre-pleura, pleura, and the artifactual region. As a LUS region is quantified from a multifrequency image at 3, 4, 5, and 6 MHz, an I_{TOT} quantity is obtained from each center frequency. Consequently, an I_{TOT} region will be composed by four different I_{TOT} values as a function of center frequency, so $I_{\mathrm{TOT}}(f)$. The following equation was utilized for the computation of I_{TOT}:

$$I_{TOT_R}(f) = 20\log_{10}\left(A_{PIX}\sum_{i,j}10^{\frac{ROI_{(i,j,R)}}{20}}\right)$$

where A_{pix} is the pixel area ($3.7877\times10^{-3}\,\mathrm{mm}^2$, i and j are indices of the pixel (with intensities greater than -35 dB) included in the ROI at the i^{th} row, j^{th} column. The $ROI(i,j,R)$ is the intensity, in logarithmic scale, of the pixel at the i^{th} row, j^{th} column,[4] and R is the region selected ($R = 1,2,3$), corresponding to pre-pleura, pleura, and artifactual region. The remaining two quantities were derived from the ratios of different quantities; respectively, I_{TOT4} was derived from the ratio $I_{\mathrm{TOT1}} - I_{\mathrm{TOT2}}$, and I_{TOT5} was derived

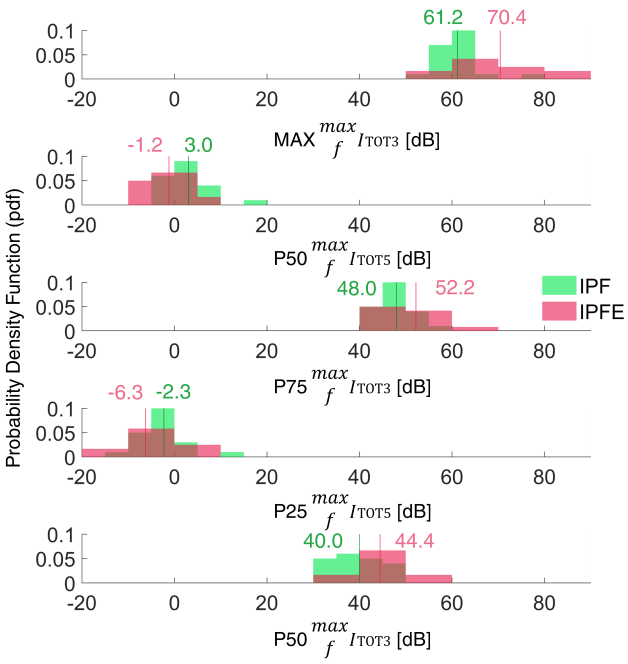

Figure 2: Probability density function (PDF) of the significant statistical parameters depicted in Tab. 1 divided by IPF (green bars) and IPFE (red bars). The mean of each PDF is depicted with a vertical line and the value with the same color.

from the ratio $I_{\mathrm{TOT2}} - I_{\mathrm{TOT3}}$ (see Fig. 1). Since $I_{\mathrm{TOT}}(f)$ is represented in logarithmic scale, by ratios we refer to the difference of two $I_{\mathrm{TOT}}(f)$ at the same center frequencies [e.g., $I_{\mathrm{TOT4}}(f = 3)$=$I_{\mathrm{TOT1}}(f = 3)$-$I_{\mathrm{TOT2}}(f = 3)$, $I_{\mathrm{TOT4}}(f = 4)$=$I_{\mathrm{TOT1}}(f = 4)$-$I_{\mathrm{TOT2}}(f = 4)$]. Although, five I_{TOT} quantities are obtained, I_{TOT1} is neglected from the analysis, as it does not provide any backscattering information from the lung. Instead, I_{TOT1} is used to compute $I_{\mathrm{TOT4}} = I_{\mathrm{TOT1}} - I_{\mathrm{TOT2}}$, which considers the signal attenuation caused by different intercostal tissue layers. From each $I_{\mathrm{TOT}}(f)$ quantity [composed by four I_{TOT}, one for each center frequency], three spectral biomarkers are extracted: center frequency, corresponding to the frequency presenting the highest I_{TOT}; bandwidth, which corresponds to the range of frequencies in the multifrequency image within $-6\,\mathrm{dB}$ from $\max_f I_{\mathrm{TOT}}$, and $\max_f I_{\mathrm{TOT}}$, which is the maximum I_{TOT} value obtained from an $I_{\mathrm{TOT}}(f)$. A total of 12 spectral biomarkers are obtained for each LUS image. Previously, the distribution of each spectral biomarker at the patient level was analyzed by its mean value. Here, each biomarker distribution is characterized by five different statistical parameters: minimum (MIN), 25^{th} percentile (P25), 50^{th} percentile (P50), 75^{th} percentile (P75), and maximum value (MAX), obtaining a total of 60 statistical parameter for each patient (12 spectral biomarkers $\times$ 5 statistical parameters).

D. CLASSIFICATION

A rank of the most significant statistical parameters to stratify chronic IPF and IPFE is derived by an ANOVA test with the MATLAB function “anova1”. The stratification performance of the ranked parameters is tested by means of a Naive Bayes classifier with the MATLAB function “fitcnb”. The classifier was designed following a repeated nested k-fold strategy as follows. The dataset is initially split into four folds in the outer loop; subsequently, each outer fold was split into four stratified folds in the inner loop, to guarantee an equal distribution of the two classes and avoid bias during the training phase. In the inner fold, hyperparameters of the model were optimized and tested in the outer fold. Each analysis was repeated

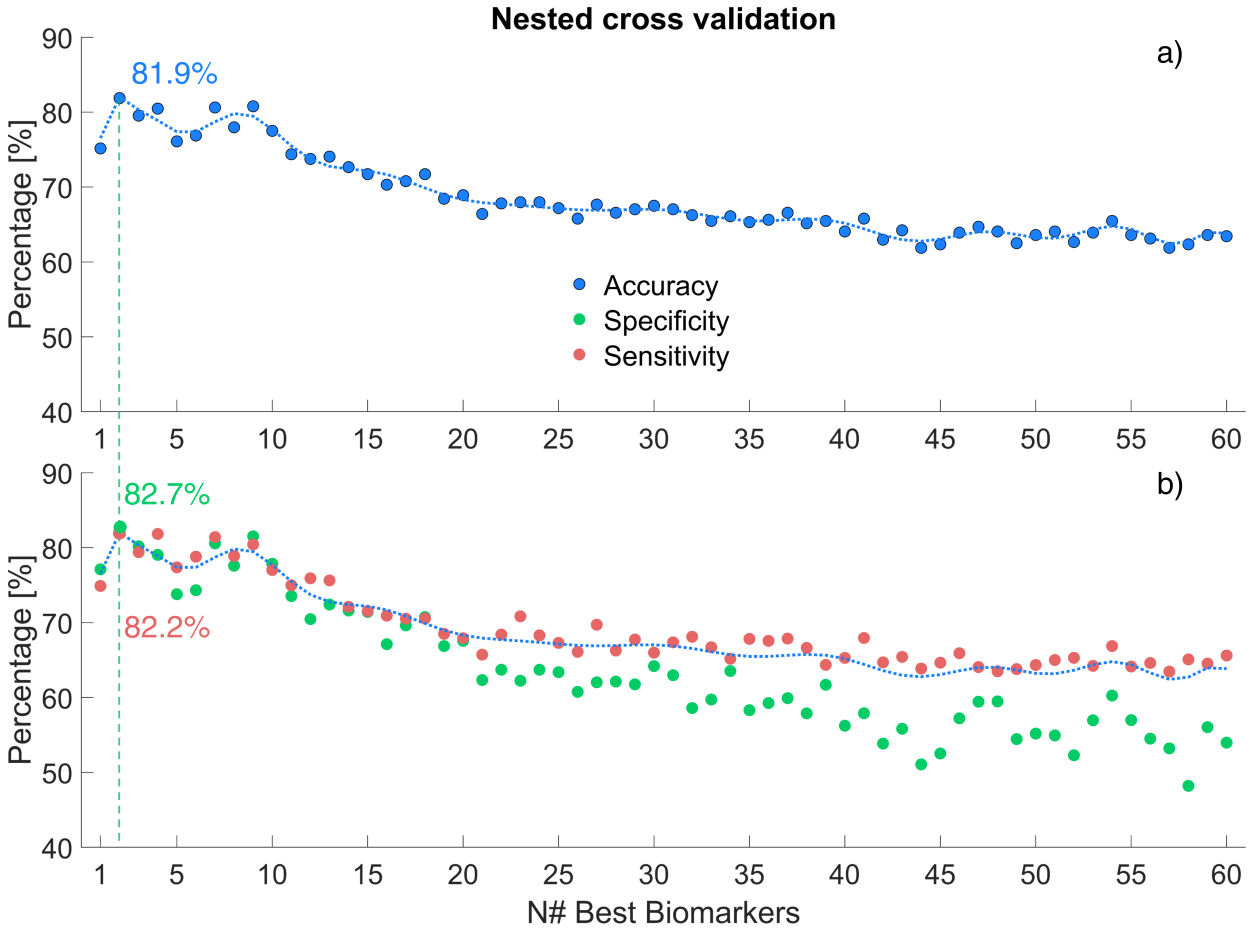

Figure 3: Classification performance in terms of: a), accuracy (blue dots), and b), specificity (green dots) and sensitivity (red dots). The blue line is the curve fitted on the accuracy values, while the green line represents the number of input parameters leading to best accuracy and the respective sensitivity and specificity (specified in percentage with the respective metric colors).

20 times to further guarantee the robustness of the analysis. To determine the optimal number of input parameters, classifiers were trained using an incremental input approach (starting from the most significant parameter in Tab. 1, incrementally adding parameters until all 60 were used).

Stratification performance was assessed in terms of accuracy, sensitivity, and specificity. Accuracy is associated to the amount of correctly classified patients, whereas sensitivity and specificity measure the performance in classifying positive and negative cases, respectively. Given a confusion matrix composed by true positive (*TP*), true negative (*TN*), false positive (*FP*), and false negative (*FN*) predictions, accuracy, sensitivity, and specificity were derived as follow:

$$Accuracy = \frac{TP+TN}{TP+TN+FP+FN}; \qquad Sensitivity = \frac{TP}{TP+FN}; \qquad Specificity = \frac{TN}{TN+FP}$$

Specifically, for each metric, the 20 values obtained from repeated cross-validation were averaged.

To compare the stratification performance of the proposed approach with SoA approach, the same classification pipeline was used with the mean value of the spectral biomarkers presented in SoA.[19]

Table 2: Parameters rank from SoA, consisting on the biomarker mean value. p-values are highlighted by a color map from green (significant) to red (non-significant).

I_{TOT2}		I_{TOT3}		I_{TOT4}		I_{TOT5}	
Qty.	*p-value*	Qty.	*p-value*	Qty.	*p-value*	Qty.	*p-value*
maxI	0.8229	**maxI**	0.0486	**maxI**	0.0794	**maxI**	0.0155
CF	0.5199	**CF**	0.7224	**CF**	0.4494	**CF**	0.5958
BW	0.8034	**BW**	0.9410	**BW**	0.3645	**BW**	0.2157

Abbreviations: MaxI = $\max_f I_{\mathrm{TOT}}$; CF = Center Frequency; BW = Bandwidth.

3. RESULTS

Table 1 illustrates the rank of the most significant statistical parameters obtained (p-value<0.05 highlighted in green). The probability density function (PDF) of the significant parameters are depicted in Fig. 2. The most significant parameter, with a p-value of 0.0012, is MAX $\max_f I_{\mathrm{TOT3}}$, which correspond to the artifactual region; PDFs present mean values of $61.2\,\mathrm{dB}$ and $70.4\,\mathrm{dB}$ for chronic IPF and IPFE, respectively.

Figure 3 depicts the results of the Naive Bayes classifier trained by increasing the number of statistical parameters from the most significant to the less significant (see Tab. 1). The most effective number of parameters in terms of accuracy (blue dots) is 2 (pointed by the vertical green line), in which the classifiers present a mean accuracy of 81.9% with sensitivity and specificity levels of 82.2% and 82.7%, respectively. The blue curve represents a 20^{th} order polynomial fitted to the accuracy values, illustrating how increasing the number of parameters worsens the accuracy.

Table 2 illustrates the rank of the most significant parameters (p-value<0.05 highlighted in green) obtained from the mean of the spectral biomarkers presented in SoA.[19] Only two parameters are significant, with values of 0.0155 and 0.0486 for $\max_f I_{\mathrm{TOT}}$ of I_{TOT5} and I_{TOT3}, respectively.

Figure 4 shows the classification performance of the SoA parameters, with accuracy levels up to 68.9%, and sensitivity and specificity of 70.0% and 68.7%, respectively.

4. DISCUSSION AND CONCLUSION

Q-LUS approaches have been developed to address key limitations of standard LUS, in particular, the limited reproducibility and specificity, while preserving safety and real-time imaging. Previous studies have demonstrated the ability of Q-LUS spectral biomarkers to differentiate different pathologies. However, for each patient, the information contained in each biomarker distribution was compressed into a mean value. In this study, LUS images were automatically segmented using ASAP[19] into three regions and quantified by means of 12 spectral biomarkers. Rather than characterizing each biomarker distribution by the mean value (SoA approach),[19] we extracted five statistical parameters. The stratification capability of the obtained parameters was then evaluated with a Naïve Bayes classifier, to distinguish between two IPF histological stages.

Results demonstrate that a more accurate analysis of each spectral biomarker distribution, compared with SoA approach, improves the stratification potential of Q-LUS and its specificity. Indeed, while SoA approach presents only two significant parameters, the proposed approach extracts five significant parameters and improves IPF stratification of +13% of accuracy, +12.2% sensitivity, and +14% specificity. Best performance are achieved using between 2 to 10 parameters.

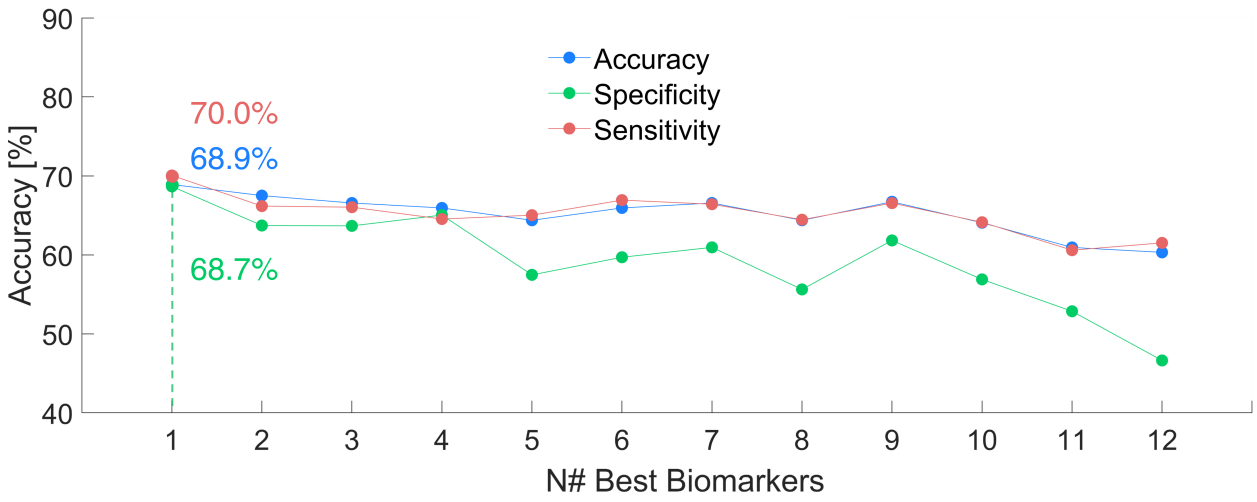

Figure 4: Classification performance of the SoA parameters in terms of: accuracy (blue dots), specificity (green dots), and sensitivity (red dots). The blue line is the curve fitted on the accuracy values, while the green line represents the number of input parameters with the best accuracy and the respective sensitivity and specificity (specified in percentage with the respective metric colors).

The spectral biomarkers that exhibit significant statistical parameters are $\max_f I_{\mathrm{TOT}}$ of the artefactual region and I_{TOT4} (obtained as the difference between I_{TOT} of PL and I_{TOT} of the artifactual area). These results may reflect the relationship between Q-LUS parameters and IPF and IPFE imaging patterns as two distinct conditions. Respectively: an heterogeneous and chronic progression of damaged lung anatomy, cystic air-spaces formation, and sparse inflammatory infiltrates (lymphocytes and plasma cells) for IPF;[1] an acute exacerbation of the diffuse alveolar damage with a prominent hyperplasia, squamous metaplasia, interstitial infiltration of myofibroblasts, and early collagen deposition for IPFE.[3] These pathological differences could lead IPFE to exibit a higher concentration of more intense LUS artefactual components than IPF, resulting in Q-LUS statistical parameters with significantly different I_{TOT} values (as depicted in Fig. 2).

The dataset presents some limitations, as the cohort of patients is limited and it requires an increment on the patients number to confirm the robustness of the analysis. Additionally, despite chronic IPF and IPFE classes were not ideally balanced, this limitation was addressed by training the classification models with a repeated nested k-fold strategy that utilizes a balanced split of the two classes.

Coherently with the proposed approach, SoA approach presents as the most significant spectral biomarker the statistical parameters of $\max_f I_{\mathrm{TOT}}$ of I_{TOT5}.

In this study, we verified whereas extracting more statistical values across the biomarker distributions impacts on IPF stratification performance. Indeed, while previous studies approximated the distribution on one single value (mean), here we extracted five different statistical parameters (MIN, P25, P50, P75, and MAX) to analyse how values are spread across the distributions. Although this subset of parameters represents only a subgroup of the available statistics that can be utilised, results demonstrate significant IPF stratification improvements. In future studies, we will investigate whether the use of additional statistical parameters (e.g., variance and skewness) could further improve the performance of the approach.

Moreover, longitudinal LUS data could be acquired from the same population to further test the monitoring potential of Q-LUS over the evolution of pathological stages.

ACKNOWLEDGMENTS

This work was partially supported by a research grant provided in compliance with Mission 6/component 2/Investment: 2.1 ”Strengthen-ing and enhancing biomedical research in the NHS”, financed by the European Union - NextGenerationEU, CUP: E63C24000660007.

REFERENCES

[1] Talmadge E King, Annie Pardo, and Moisés Selman. Idiopathic pulmonary fibrosis. *The Lancet*, 378(9807):1949–1961, 12 2011.

[2] Harold R. Collard, Christopher J. Ryerson, Tamera J. Corte, Gisli Jenkins, Yasuhiro Kondoh, David J. Lederer, Joyce S. Lee, Toby M. Maher, Athol U. Wells, Katerina M. Antoniou, Juergen Behr, Kevin K. Brown, Vincent Cottin, Kevin R. Flaherty, Junya Fukuoka, David M. Hansell, Takeshi Johkoh, Naftali Kaminski, Dong Soon Kim, Martin Kolb, David A. Lynch, Jeffrey L. Myers, Ganesh Raghu, Luca Richeldi, Hiroyuki Taniguchi, and Fernando J. Martinez. Acute Exacerbation of Idiopathic Pulmonary Fibrosis. An International Working Group Report. *American Journal of Respiratory and Critical Care Medicine*, 194(3):265–275, 8 2016.

[3] Harold R. Collard, Bethany B. Moore, Kevin R. Flaherty, Kevin K. Brown, Robert J. Kaner, Talmadge E. King, Joseph A. Lasky, James E. Loyd, Imre Noth, Mitchell A. Olman, Ganesh Raghu, Jesse Roman, Jay H. Ryu, David A. Zisman, Gary W. Hunninghake, Thomas V. Colby, Jim J. Egan, David M. Hansell, Takeshi Johkoh, Naftali Kaminski, Dong Soon Kim, Yasuhiro Kondoh, David A. Lynch, Joachim Müller-Quernheim, Jeffrey L. Myers, Andrew G. Nicholson, Moisés Selman, Galen B. Toews, Athol U. Wells, and Fernando J. Martinez. Acute Exacerbations of Idiopathic Pulmonary Fibrosis. *American Journal of Respiratory and Critical Care Medicine*, 176(7):636–643, 10 2007.

[4] Federico Mento, Gino Soldati, Renato Prediletto, Marcello Demi, and Libertario Demi. Quantitative Lung Ultrasound Spectroscopy Applied to the Diagnosis of Pulmonary Fibrosis: The First Clinical Study. *IEEE Transactions on Ultrasonics, Ferroelectrics, and Frequency Control*, 67(11):2265–2273, 11 2020.

[5] Libertario Demi, Frank Wolfram, Catherine Klersy, Annalisa De Silvestri, Virginia Valeria Ferretti, Marie Muller, Douglas Miller, Francesco Feletti, Marcin Wełnicki, Natalia Buda, Agnieszka Skoczylas, Andrzej Pomiecko, Domagoj Damjanovic, Robert Olszewski, Andrew W. Kirkpatrick, Raoul Breitkreutz, Gebhart Mathis, Gino Soldati, Andrea Smargiassi, Riccardo Inchingolo, and Tiziano Perrone. New International Guidelines and Consensus on the Use of Lung Ultrasound. *Journal of Ultrasound in Medicine*, 42(2):309–344, 2 2023.

[6] Libertario Demi. Lung ultrasound: The future ahead and the lessons learned from COVID-19. *The Journal of the Acoustical Society of America*, 148(4):2146–2150, 10 2020.

[7] Federico Mento, Umair Khan, Francesco Faita, Andrea Smargiassi, Riccardo Inchingolo, Tiziano Perrone, and Libertario Demi. State of the Art in Lung Ultrasound, Shifting from Qualitative to Quantitative Analyses. *Ultrasound in Medicine & Biology*, 48(12):2398–2416, 12 2022.

[8] Federico Mento, Matteo Perini, Ciro Malacarne, and Libertario Demi. Ultrasound multifrequency strategy to estimate the lung surface roughness, in silico and in vitro results. *Ultrasonics*, 135:107143, 12 2023.

[9] Federico Mento, Mattia Perpenti, Giuliana Barcellona, Tiziano Perrone, and Libertario Demi. Quantitative Lung Ultrasound Spectroscopy Classification Performance in Differentiating CPE, Pneumonia, and PF,

a Comparative Classifiers' Analysis. In *2024 IEEE Ultrasonics, Ferroelectrics, and Frequency Control Joint Symposium (UFFC-JS)*, pages 1–4. IEEE, 9 2024.

[10] Libertario Demi, Thomas Egan, and Marie Muller. Lung Ultrasound Imaging, a Technical Review. *Applied Sciences*, 10(2):462, 1 2020.

[11] Libertario Demi, Federico Mento, Antonio Di Sabatino, Anna Fiengo, Umberto Sabatini, Veronica Narvena Macioce, Marco Robol, Francesco Tursi, Carmelo Sofia, Chiara Di Cienzo, Andrea Smargiassi, Riccardo Inchingolo, and Tiziano Perrone. Lung Ultrasound in COVID-19 and Post-COVID-19 Patients, an Evidence-Based Approach. *Journal of Ultrasound in Medicine*, 41(9):2203–2215, 9 2022.

[12] Andrea Smargiassi, Gino Soldati, Elena Torri, Federico Mento, Domenico Milardi, Paola Del Giacomo, Giuseppe De Matteis, Maria Livia Burzo, Anna Rita Larici, Maurizio Pompili, Libertario Demi, and Riccardo Inchingolo. Lung Ultrasound for COVID-19 Patchy Pneumonia. *Journal of Ultrasound in Medicine*, 40(3):521–528, 3 2021.

[13] Mattia Perpenti, Federico Mento, Sajjad Afrakhteh, Giuliana Barcellona, Tiziano Perrone, and Libertario Demi. A Novel Empirical Wavelet Transform Approach for Classification of Radiofrequency Lung Ultrasound Signals Applied to Diagnosis of Lung Diseases. In *2024 IEEE Ultrasonics, Ferroelectrics, and Frequency Control Joint Symposium (UFFC-JS)*, pages 1–4. IEEE, 9 2024.

[14] Chiara Zangrandi, Federico Mento, Mattia Perpenti, Giovanni Pierro, Alessandro Perrotta, Tiziano Perrone, Andrea Smargiassi, Riccardo Inchingolo, and Libertario Demi. Novel velocity model for the quantitative characterization of pleural sliding, in vivo multicenter clinical study on RF lung ultrasound data. *Computers in Biology and Medicine*, 209, 6 2026.

[15] Federico Mento and Libertario Demi. Dependence of lung ultrasound vertical artifacts on frequency, bandwidth, focus and angle of incidence: An in vitro study. *The Journal of the Acoustical Society of America*, 150(6):4075–4082, 12 2021.

[16] Libertario Demi, Marcello Demi, Renato Prediletto, and Gino Soldati. Real-time multi-frequency ultrasound imaging for quantitative lung ultrasound – first clinical results. *The Journal of the Acoustical Society of America*, 148(2):998–1006, 8 2020.

[17] Federico Mento, Mattia Perpenti, Giuliana Barcellona, Tiziano Perrone, and Libertario Demi. Lung Ultrasound Spectroscopy Applied to the Differential Diagnosis of Pulmonary Diseases: An In Vivo Multicenter Clinical Study. *IEEE Transactions on Ultrasonics, Ferroelectrics, and Frequency Control*, 71(10):1217–1232, 10 2024.

[18] Mattia Perpenti, Federico Mento, Giovanni Pierro, Alessandro Perrotta, Andrea Smargiassi, Riccardo Inchingolo, and Libertario Demi. Novel Quantitative Lung Ultrasound Spectroscopy Approach for Diseases Classification. In *2024 IEEE Ultrasonics, Ferroelectrics, and Frequency Control Joint Symposium (UFFC-JS)*, pages 1–4. IEEE, 9 2024.

[19] Mattia Perpenti, Federico Mento, Giovanni Pierro, Alessandro Perrotta, Tiziano Perrone, Andrea Smargiassi, Riccardo Inchingolo, and Libertario Demi. Fully automated Quantitative Lung Ultrasound spectroscopy for the differential diagnosis of lung diseases: The first multicenter in-vivo clinical study. *Computers in Biology and Medicine*, 200:111365, 1 2026.

[20] Perpenti Mattia, Eleonora Balzani, Federico Mento, Claudia Marinaro, Giacomo Bellani, Tiziano Perrone, and Libertario Demi. Quantitative Lung Ultrasound Spectroscopy: First Comparison with Gold Standard Computed Tomography Scan and Standard Lung Ultrasound for Diagnosis of Pneumonia versus Cardiogenic Pulmonary Edema. *The Ultrasound Journal*, 2026.

[21] P. Tortoli, L. Bassi, E. Boni, A. Dallai, F. Guidi, and S. Ricci. ULA-OP: an advanced open platform for ultrasound research. *IEEE Transactions on Ultrasonics, Ferroelectrics and Frequency Control*, 56(10):2207–2216, 10 2009.

[22] Federico Mento and Libertario Demi. On the influence of imaging parameters on lung ultrasound B-line artifacts, in vitro study. *The Journal of the Acoustical Society of America*, 148(2):975–983, 8 2020.

[23] Gino Soldati, Andrea Smargiassi, Riccardo Inchingolo, Danilo Buonsenso, Tiziano Perrone, Domenica Federica Briganti, Stefano Perlini, Elena Torri, Alberto Mariani, Elisa Eleonora Mossolani, Francesco Tursi, Federico Mento, and Libertario Demi. Proposal for International Standardization of the Use of Lung Ultrasound for Patients With COVID-19. *Journal of Ultrasound in Medicine*, 39(7):1413–1419, 7 2020.